Dalton Transactions

An international journal of inorganic chemistry

www.rsc.org/dalton

Volume 42 | Number 32 | 28 August 2013 | Pages 11329–11732

ISSN 1477-9226

RSC Publishing

COVER ARTICLE

Frenking, Wilson, Dutton *et al.*

Beryllium chemistry the safe way: a theoretical evaluation of low oxidation state beryllium compounds

1477-9226(2013)42:32;1-L

Dalton Transactions

RSC Publishing

PAPER

View Article Online
View Journal | View Issue

Cite this: *Dalton Trans.*, 2013, **42**, 11375

Beryllium chemistry the safe way: a theoretical evaluation of low oxidation state beryllium compounds†

Shannon A. Couchman,[a] Nicole Holzmann,[b] Gernot Frenking,*[b] David J. D. Wilson*[a] and Jason L. Dutton*[a]

Received 1st March 2013,
Accepted 2nd April 2013

DOI: 10.1039/c3dt50563d

www.rsc.org/dalton

A theoretical study of compounds containing Be in the +1 or 0 oxidation state has been carried out. The molecules considered containing Be in the +1 oxidation state are analogues of the important Mg(I)–Mg(I) dimer supported by the β-diketiminate ligand. The molecules in the 0 oxidation state are NHC supported compounds analogous to "molecular allotropes" which has recently become a topic of importance in p-block chemistry. In this case, our results demonstrate that the Be(0) complexes are far more stable than the analogous Mg(0) complexes, highlighting the opportunities afforded in Be chemistry, despite the challenges presented by the toxicity of Be compounds.

Introduction

Beryllium chemistry is underdeveloped due to the toxicity of compounds containing this element.[1] This property unfortunately conflicts with the fact that molecular beryllium chemistry is predicted to be the richest amongst the alkaline earth metals due to its greater tendency for covalent bonding.[2] Recent experimental studies give evidence for the rich and versatile chemistry of beryllium, which is largely unexplored.[3–6] Computational chemistry offers a much safer way of "performing" beryllium chemistry and predicting new molecules – *in silico*. In this manner, particularly interesting beryllium compounds can be investigated efficiently and in a convenient manner.[7,8]

A recent major advance in alkaline earth chemistry was the isolation of Mg(I) compounds containing Mg–Mg bonds by Jones and co-workers, stabilized by guanidinate or β-diketiminate (Nac–Nac) ligands such as **1Mg^{dipp}**.[9] This remarkable class of molecules has found use as a powerful, soluble reducing agent.[10,11] We became interested if this class of molecules could be extended to beryllium, and if so, what properties and bonding characteristics these compounds might possess. In this context we have carried out an *a priori* computational investigation of two classes of unknown low-valent beryllium compounds containing Be–Be bonds. The first class of compounds are Be(I) complexes (**1Be^{R}**) directly analogous to the Mg(I) species **1Mg^{dipp}** reported by Jones.

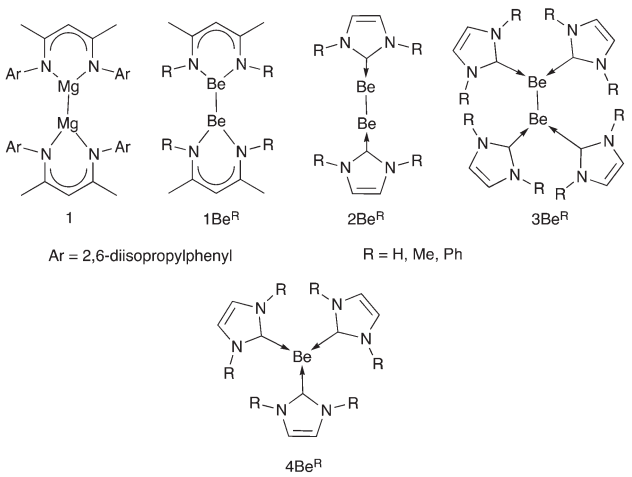

The second class is Be(0) compounds ligated by *N*-heterocyclic carbenes (NHCs), **2Be^{R}**, **3Be^{R}**, **4Be^{R}**. The use of NHCs to stabilize highly reactive molecular "allotropes" in an L–E$_n$–L framework is currently an area of major interest.[12,13] Examples of L–E$_n$–L compounds have recently been synthesized for Si_2,[14] Ge_2,[10] Sn_2,[15] P_2,[16] and As_2.[17] Dicarbon, B_2 and the heavy group 14/15 species have been considered theoretically.[18–20] Frenking and Jones' prediction of NHC stabilized B_2 has recently been realized.[21] The C(0) carbodicarbene (NHC–C–NHC) is another example in this area of theoretical prediction leading

[a]*La Trobe Institute for Molecular Science, Department of Chemistry, La Trobe University, Melbourne, Victoria, Australia. E-mail: david.wilson@latrobe.edu.au, j.dutton@latrobe.edu.au; Tel: +61 (0)3 94793213*
[b]*Fachbereich Chemie, Philipps-Universität Marburg, 35032 Marburg, Germany. E-mail: frenking@chemie.uni-marburg.de; Fax: (+49) 6421-2825566*

†Electronic supplementary information (ESI) available: Cartesian coordinates for all molecules, geometries and MOs for derivatives not featured in main text. See DOI: 10.1039/c3dt50563d

experimental confirmation.[22,23] The concept of using strong neutral Lewis bases to stabilize molecular "allotropes" has not yet been extended to the s-block of elements. Diberyllium (Be_2) is a molecule that has long fascinated theoretical and experimental chemists alike. Simple MO theory predicts a bond order of zero. Recent high-profile experimental and theoretical studies have found a distinct bonding interaction of 9.4 kJ mol^{-1} (exp.) and 11.2 kJ mol^{-1} (calc.) with a Be–Be distance of approximately 2.5 Å, which is not considered a traditional covalent bond.[24,25] In light of the unexplored yet rich chemistry of beryllium, it is of interest to investigate whether the Be atom or Be_2 molecule can be stabilised by donor ligands as is the case for p-block elements. One of the features that renders NHC ligated Be_2 an attractive target is that reasonable starting compounds are already known in the form of NHC adducts of $BeCl_2$ or $[BeCl]^+$.[26,27] NHCs are also attractive since they offer kinetic stability due to the potential to incorporate bulky R groups providing steric shielding.[28,29]

Results and discussion

Be(I) β-diketiminate dimers

Geometry optimizations were carried out at the B3LYP/def2-TZVPP level of theory. Substitution of Mg for Be in the Nac–Nac framework (**1Be^{Me}**, Fig. 1) resulted in a slight contraction of the chelate and the formation of a less distorted 6-member ring. For **1Be^{Me}**, the Be–Be and Be–N bond distances were calculated to be 2.162 and 1.670 Å, respectively (**1Be^{Ph}**: 2.134 and 1.689 Å).[30] The Be–Be distance is consistent with reported calculations of comparable compounds, also using anionic or dianionic ligands (*e.g.* Cp, reduced diimines).[7,8,31]

The Wiberg bond index (WBI) for the Be–Be bond was calculated to be 0.954 in **1Be^{Me}** and 0.917 in **1Be^{Ph}**, consistent with a single bond. The WBI values are higher than calculated for the analogous Mg species, **1Mg^{Me}** (**1Mg^{Me}** Mg–Mg 2.875 Å, WBI = 0.780; **1Mg^{Ph}** Mg–Mg 2.847 Å, WBI 0.772). In **1Be^{R}** a Be–Be sigma bond dominates the HOMO of the molecule; the HOMO − 1 and the LUMO are both ligand based. The HOMO–LUMO gap is 3.15 eV, which compares with 3.18 eV for the known, isolated compound **1Mg^{dipp}**. A cursory examination of standard reduction potentials for $M^{2+} \rightarrow M^0$ indicates that the Be complex (−1.85 V) is likely to be a weaker reducing agent than the analogous Mg complex (−2.37 V), reducing its synthetic utility, especially given the challenges of working with Be. Conversely, this property may also make **1Be^{R}** more stable than **1Mg^{dipp}** with respect to REDOX reactions, although in an account focusing on the related Mg compounds, it was indicated that an attempted synthesis of the Be analogue failed (using **1Mg^{dipp}** as a reducing agent).[32] A recent report from Hill and co-workers using NacNac ligands substituted with methyl groups in the ligand backbone observed H-atom abstraction from the methyl groups upon attempted reduction of a Be(II) precursor complex.[33] It should also be emphasized that using the reduction potential for M^{2+} only gives an expected trend for these alkaline earth +1 species. For **1Be^{Me}** and **1Be^{Ph}**, the Be–Be bond dissociation energy was calculated to be 188.6 and 250.0 kJ mol^{-1}, respectively (MP2/def2-TZVPP//B3LYP/def2-TZVPP). This compares to 188 kJ mol^{-1} calculated for the Mg–Mg bond in compound **1Mg^{dipp}**.[32] Related theoretical studies on Be–Be bonds in $[Be_2]^{4+}$ fragments bound by reduced diimine ligands were calculated to have Be–Be dissociation energies of 122 kJ mol^{-1}.[7]

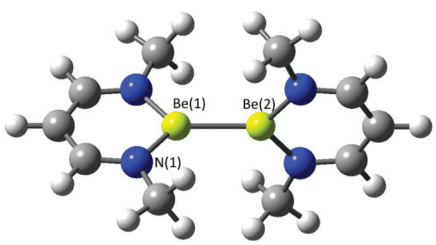

Fig. 1 Optimized geometry of **1Be^{Me}**. Selected bond distances (Å): Be(1)–Be(2) 2.162, Be(1)–N(1) 1.670.

Beryllium(0) dimers

The apparent viability of the Be(I)–Be(I) complex stabilized by the Nac–Nac ligand (**1Be^{R}**) led us to consider the possibility of a Be(0)–Be(0) complex bound by neutral ligands. An older theoretical study used CO as a ligand and found a structure with a very short (1.938 Å) Be–Be bond in a $(CO)_2$–Be═Be–$(CO)_2$ motif with a Be–Be π bond.[34] However, the calculated facile dissociation of CO from this compound (B3LYP/def2-TZVPP), and the lack of suitable starting materials, likely make this molecule synthetically unviable. A study by another group was able to observe these and other CO adducts of Be and Be_2 spectroscopically *via* low temperature matrix isolation methods.[35] The view of a strong Be═Be double bond in this molecule was challenged in subsequent theoretical studies, for which a delocalized, multi-centred Be–Be bonding environment was considered more appropriate.[36,37] B3LYP/def2-TZVPP MO calculations indicate that a Be–Be σ bond dominates the HOMO − 1, while the LUMO is a π* orbital primarily based on the N–C NHC bonds, with some coefficient in the C–Be bond. The Be–C σ bonds are evident in a pair of nearly degenerate orbitals in the HOMO − 6 and HOMO − 7. For the $(CO)_2$–Be–Be–$(CO)_2$ complex the 3c–2e Be–Be–C bond order index is calculated to be 0.114 (B3LYP/def2-TZVPP; the theoretical maximum 3c–2e index is 0.296), which is indicative of some delocalisation and 3c–2e bond character. Irrespective of the bonding situation, previous studies indicate that by using a donor ligand L it might be possible to induce genuine Be–Be bonds in complexes L_n–Be–Be–L_n.

Optimized geometries

Geometry parameters for all calculated species are collected in Table 1; geometries of species not featured in the manuscript are found in the ESI.† In all cases both singlet and triplet multiplicities were considered; unless noted the following discussion relates to the lower energy singlet state species. Geometries were optimized with B3LYP-DFT using both def2-TZVP

Table 1 DFT optimized geometrical parameters for compounds **2E^R–4E^R** (E = Be, Mg; R = H, Me, Ph)[a]

	R = H	Me	Ph	H	Me	Ph	Me	Ph
Beryllium		**2Be^R**			**3Be^R**		**4Be^R**	
r(Be–Be)	1.945	1.949 (1.316)	1.978 (1.134)	2.12	2.098 (0.990)	2.211 (0.462)	—	—
r(Be–C)	1.683	1.687 (0.717)	1.686 (0.684)	1.73	1.754 (0.657)	1.769 (0.222)	1.727 (0.865)	1.750 (0.812)
r(C–N)	1.383	1.378	1.393	1.374	1.384	1.397	1.391	1.400
θ(Be–Be–C)	180.0	180.0	178.4	118.8	126.9	126.0	—	—
θ(C–Be–Be–C)	180.0	0.0	26.2	180.0	176.4	178.4	—	—
θ(C–Be–C)	—	—	—	119.8	114.7	120.7	120.1	120.0
Magnesium		**2Mg^R**			**3Mg^R**		**4Mg^R**	
r(Mg–Mg)	3.345	3.069 (0.756)	2.961 (0.284)	3.163	2.946 (1.194)	[b]	[b]	[b]
r(Mg–C)	2.380	2.384 (0.245)	2.291 (0.190)	2.307	2.309 (0.346)	[b]	[b]	[b]
r(C–N)	1.353	1.361	1.375	1.357	1.366	[b]	[b]	[b]
θ(Mg–Mg–C)	91.1	107.9	121.0	97.5	122.0	[b]	[b]	[b]
θ(C–Mg–Mg–C)	180.0	180.1	180.0	180.0	174.5	[b]	[b]	[b]

[a] B3LYP/def2-TZVPP results except for R = Ph, for which B3LYP/def2-TZVP results are tabled. Bond distances (*r*) in units of Å, angles (*θ*) in degrees. Wiberg bond indices (WBIs) in parentheses. [b] No stable minima located.

and def2-TZVPP basis sets, which produced very similar geometries. For the larger molecular systems with multiple ligands and R = Ph, only B3LYP/def2-TZVP optimized geometries are reported.

For L–Be_2–L a number of molecular conformations were considered. The lowest energy L–Be–Be–L structure (singlet state multiplicity) that retains a distinct Be_2 core exhibits a linear C–Be–Be–C arrangement with co-planar NHC-ligands (**2Be^{Me}**, Fig. 2) and possesses D_{2h} symmetry. For **2Be^{Me}** the Be–Be bond distance is calculated to be 1.949 Å (**2Be^{Ph}**; 1.978 Å), significantly shorter than the distance found in the free Be_2 dimer at 2.509 Å[21,22] and also shorter than 2.162 and 2.134 Å calculated for the Nac–Nac complexes **1Be^{Me}** and **1Be^{Ph}**, respectively. In **2Be^{Me}** the Be–C bond distance is 1.687 Å, slightly shorter than the 1.74–1.80 Å observed in isolated NHC–$BeCl_n$ adducts and related compounds.[4,26,27,38] The Be–C WBI of 0.72 and 0.80 in **2Be^{Me}** and **2Be^{Ph}**, respectively, compares to 0.22 in the recently reported NHC–$BeCl_2$ adduct.[27]

For **2Be^{Me}** and **2Be^{H}**, the triplet state is lower in energy than the singlet state by 9.1 and 3.2 kJ mol^{-1}, respectively (Δ*G* values, SCS-MP2/def2-TZVPP//B3LYP/def2-TZVPP; the E_e values are 3.4 and −8.0 kJ mol^{-1}, respectively). For **2Be^{Ph}**, the singlet–triplet energy gap is *ca.* 50 kJ mol^{-1}, which may be considered a more synthetically relevant system, and so for the following discussion only the singlet state structure is considered.

Using a Be_2 fragment orthogonal to the ligands as a starting point revealed an alternative geometry (**2Be^{Me}(B)**; Fig. 3), which is 29.5 kJ mol^{-1} lower in energy than **2Be^{Me}** (Δ*G* value, MP2/def2-TZVPP//B3LYP/def2-TZVPP). The structure no longer resembles the L–E_2–L structure, but features a 4-membered "butterfly" Be–Be–C–N ring, where one NHC coordinates in a classic fashion to Be(1), while Be(2) and the other NHC become involved in a bridging interaction, substantially elongating the involved C–N bond (1.535 Å). The Be–Be bond in this conformation is 1.931 Å. The "normal" NHC–Be bond, Be(1)–C(1), is 1.72 Å, while the contacts with the NHC involved in the ring are Be(2)–C(2) 1.834 Å, B(1)–C(2) 1.654 Å and Be(2)–N(1) 1.640 Å. It is suggested that **2Be^{Me}(B)** is an intermediate

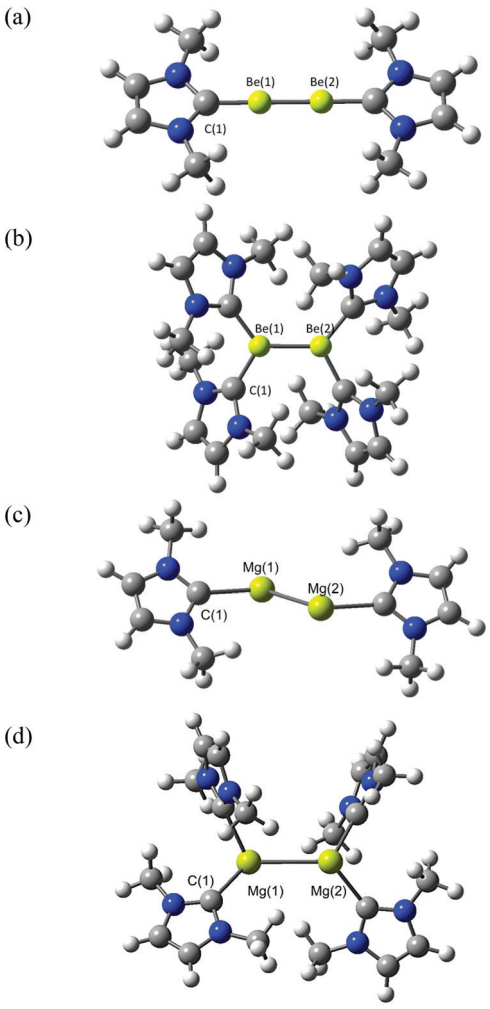

Fig. 2 Optimized geometries of (a) **2Be^{Me}**, (b) **3Be^{Me}**, (c) **2Mg^{Me}** and (d) **3Mg^{Me}**.

on the potential energy surface of the insertion reaction of Be into the NHC ring. The tendency for Be to activate the CN bond in an NHC ring and insert itself into the ring has

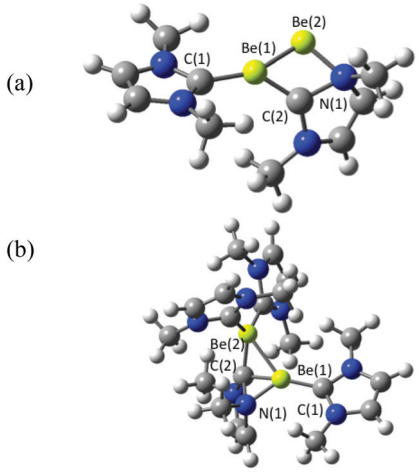

Fig. 3 Optimized geometries of (a) **2Be^{Me}(B)** and (b) **3Be^{Me}(B)**. Selected bond distances (Å): (a) Be(1)–Be(2) 1.931, C(1)–Be(1) 1.720, C(2)–Be(1) 1.654, C(2)–Be(2) 1.834, Be(2)–N(1) 1.640, C(2)–N(1) 1.535. (b) Be(1)–Be(2) 2.254, C(1)–Be(1) 1.706, C(2)–Be(2) 1.727, C(2)–Be(1) 1.741, C(2)–N(1) 1.548.

previously been noted, although the mechanism is not known.[39] We are currently investigating the mechanism and energetics of ring insertion, which will be reported in a separate publication. For the purpose of the current discussion, the bridged system is not considered further. Although **2Be^{Me}** is not the global minimum, it is a minimum on the potential energy surface and so analysis of its bonding and electronic structure is thus relevant and justified for comparison with other L–E_2–L species, which is the focus of the present paper. Also, it can be expected that more bulky substituents of **2Be^{R}**, which are often used in synthesis, will shift the relative energy of **3Be^{R}** and **4Be^{R}** toward the former species.

Substitution of the Be in **2Be^{R}** for Mg (**2Mg^{R}**; NHC^{R}–Mg–Mg–NHC^{R}) resulted in a similar linear L–E_2–L geometry, with Mg–Mg and Mg–C bonds both longer than the Be analogue, as expected for the larger atom. However, analysis of the vibrational frequencies indicated that the Mg species in this conformation is not a true minimum, with a negative vibration dominated by an Mg–Mg bond. Conformational analysis revealed a *trans*-bent C–Mg–Mg–C arrangement to be the minimum energy geometry (C_i symmetry).[40] In the *trans* configuration the Mg–Mg bond is quite long at 3.069 Å (*cf.* 2.875 Å in **1Mg^{dipp}**). For **2Mg^{H}**, the C–Mg–Mg angle is 91.9°. The more synthetically relevant **2Mg^{Me}** and **2Mg^{Ph}** complexes give slightly more obtuse C–Mg–Mg angles of 107.9 and 121.0°, respectively.

A tetrakis NHC_2–Be_2–NHC_2 complex, analogous to the previously considered tetrakis $(CO)_2BeBe(CO)_2$ complex, was also investigated (**3Be^{Me}**, Fig. 2). Similar to the CO complex, **3Be^{Me}** and **3Be^{Ph}** exhibit a planar geometry about the Be centres, with a Be–Be bond distance of 2.098 (**3Be^{Me}**) and 2.225 Å (**3Be^{Ph}**). Analogous to **2Be^{R}**, if an orthogonal Be–Be starting point is used for **3Be^{R}**, a conformation where the Be–Be forms a 4-membered ring with one of the NHC ligands is also found to be slightly lower in energy (**3Be^{Me}(B)**, Fig. 3). If Mg is substituted for Be in this case (**3Mg^{Me}**), the geometry distorts to pyramidal about the Mg centres with a Mg–Mg bond distance calculated to be 2.946 Å. All attempts to locate a minimum energy conformation for Mg analogues of **2Be^{R}(B)** and **3Be^{R}(B)** resulted in dissociation.

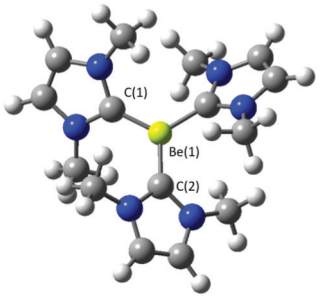

Fig. 4 Optimized geometry of **4Be^{Me}**.

Finally, given the significant interest in carbones CL_2,[41,42] we also considered a single Be(0) atom trapped by three NHC^{R} ligands, **4Be^{R}** (Fig. 4). This species was also described in a very recent paper;[43] our results are consistent with those of Parameswaran *et al.*, so we limit discussion to relevant comparisons in the present study. From thermochemical studies (see next section) it is apparent that three NHCs is the optimal number of ligands to bind a single Be atom, as this completes an 8-electron octet about the Be(0) centre. The optimized structures for R = H, Me and Ph (**4Be^{R}**) revealed a planar geometry about the Be centre, with the NHCs arranged in a propeller fashion with respect to one another with C_3 symmetry (Fig. 4). The Be–C bond distances were calculated to be 1.698 (**4Be^{H}**) to 1.750 Å (**4Be^{Ph}**), with calculated Be–C WBIs of 0.812–0.865. All attempts to locate analogous Mg complexes resulted in ready dissociation of the NHCs from the bare Mg atom, and no stable geometrical minimum could be located.

Thermodynamic studies

Representative dissociation energies for the NHC complexes are collected in Table 2. Calculations regarding possible decomposition/dissociation reactions are an important consideration in determining if these predicted species are likely to be isolable in the laboratory.[44]

Thermochemical calculations indicate that **2Be^{Me}** and **2Be^{Ph}** are stable by 247.1 and 329.6 kJ mol^{-1} with respect to dissociation into Be_2 and 2 NHC^{R}, respectively (ΔG for dissociation is positive in sign). This can be compared with values ranging from 352 (E = Si) to 89 (E = As) kJ mol^{-1} for known, isolated species from groups 14–15.[20] NHC^{H}–B–B–NHC^{H} has been predicted to have a very high interaction energy of >1200 kJ mol^{-1} with respect to B_2 and 2 H_2NHC.[18] The all carbon system NHC^{R}–C–C–NHC^{R} has association values calculated to range from 584 (R = Me) to 662 (R = Ph) kJ mol^{-1}.[19] The addition of two further equivalents of NHC to **3Be^{R}** is also favourable, giving an overall stability for **4Be^{R}** of 384.1 and 380.8 kJ mol^{-1} with respect to Be_2 and 4 NHC^{R} for R = Me and Ph, respectively. Compound **2Mg^{R}** is much less

stable with respect to NHC dissociation; −13.9 kJ mol^{-1} for R = Me, and 24.2 kJ mol^{-1} for R = Ph. The addition of 2 further equivalents of NHC^{Me} giving **3Mg^{Me}** only results in a marginal (18 kJ mol^{-1}) gain in stabilization with respect to dissociation, which is also likely insufficient for a targeted isolation.

Dissociation at the Be–Be bond is also disfavoured for compounds **2Be^{R}** and **3Be^{R}**, with the calculated free energies for "dimerization" of the respective fragments of −229.4 and −270.7 kJ mol^{-1} for **2Be^{Me}** and **2Be^{Ph}**, respectively. For **3Be^{Me}** and **3Be^{Ph}**, the corresponding Be–Be association energies are −126.2 and +99.1 kJ mol^{-1}, respectively. For **3Be^{Ph}** this is consistent with the low WBI (0.462) calculated for the Be–Be bond, and indicates that **3Be^{Ph}** is a synthetically unviable molecule. The Mg–Mg bonds in **2Mg^{R}** and **3Mg^{R}** are also predicted to undergo facile dissociation; coupled with the NHC dissociation data it appears the Mg analogues are non-viable species.

For compounds **2Be^{Ph}** and **3Be^{R}** the singlet state is lower in energy than the triplet state, an important consideration if a synthesis is to be targeted. This is in contrast to the CO–Be–Be–CO system, which was calculated to have a triplet ground state. $(CO)_2$–Be–Be–$(CO)_2$ was calculated to have a singlet ground state.[35] However, calculations performed in that study indicated the dissociation of one CO to be favourable by 29.4 kJ mol^{-1}.

In **4Be^{Me}** the dissociation energy for one NHC was calculated to be 139 kJ mol^{-1}. The loss of one NHC, followed by dimerization of the NHC^{R}–Be–NHC^{R} fragment (*e.g.* eqn (4)) was calculated to be unfavourable by 89 kJ mol^{-1}. Overall the stability of **4Be^{Me}** towards dissociation to a Be atom and 3 NHCs is 224.3 kJ mol^{-1}. The free energy of the addition of 4 NHCs to **2Be^{Me}** and **2Be^{Me}(B)** giving two equivalents of **4Be^{Me}** was calculated to be −275.0 and −233.1 kJ mol^{-1}, respectively. This data indicates that in the presence of sufficient quantities of NHC^{R}, **4Be^{R}** would be the most stable entity. The singlet state for **4Be^{R}** was calculated to be lower in energy than the triplet state.

Table 2 SCS-MP2/def2-TZVPP//B3LYP/def2-TZVPP calculated Δ*G* for reactions 1–4 (units of kJ mol^{-1})

Reaction	R = H	Me	Ph
Beryllium			
1	−201.1	−247.1	−329.6
2	−359.3	−384.1	−250.2[a]
3	−166.7	−229.4	−270.7
4	−190.2	−126.2	99.1[a]
Magnesium			
1	−16.4	13.9	−24.2[b]
2	−61.1	−4.2	
3	3.5	12.8	9.1[b]
4	−190.0	−34.1	

[a] B3LYP/def2-TZVP results. [b] No stable minima located for reaction product.

(1)

(2)

$$2(R_2NHC)\text{–}E \rightarrow (R_2NHC)\text{–}E\text{–}E\text{–}(R_2NHC) \quad (3)$$

$$2(R_2NHC)_2\text{–}E \rightarrow (R_2NHC)_2\text{–}E\text{–}E\text{–}(R_2NHC)_2 \quad (4)$$

Bonding analysis

As the Be(0) complexes **2Be^{R}**, **3Be^{R}** and **4Be^{R}** were calculated to be thermodynamically viable, we undertook a closer examination of the bonding interactions in these molecules. Ligand substitution has little effect on the key frontier orbitals for the respective compounds; therefore they are described as a set, except where noted.

The bonding situation in **2Be^{Me}** (NHC^{Me}–Be_2–NHC^{Me}) shall be discussed in detail. Fig. 5 shows the most important

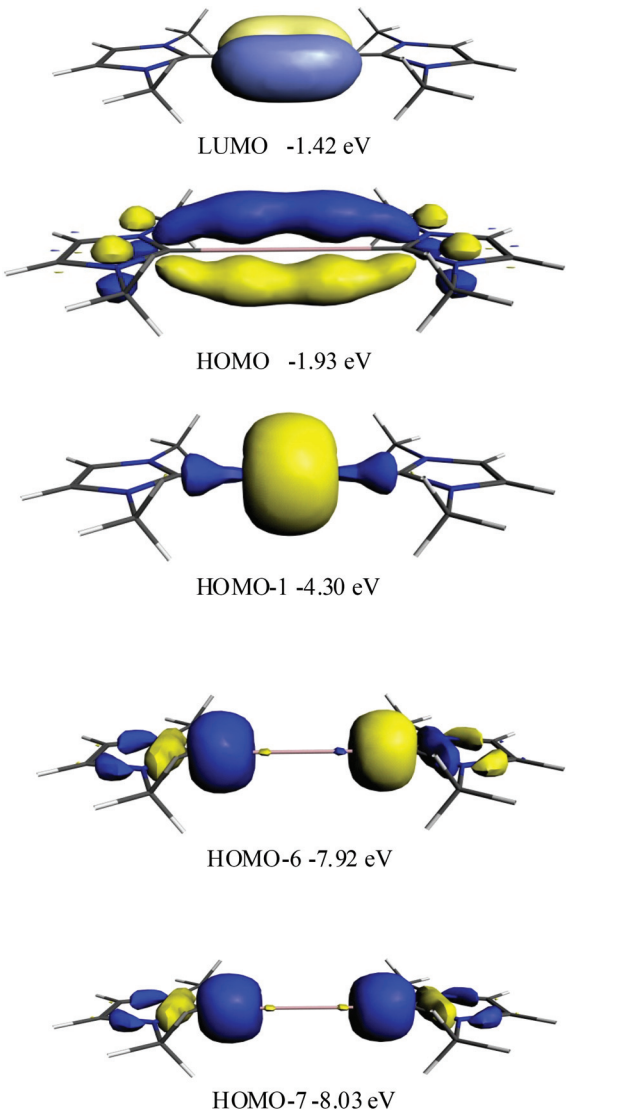

Fig. 5 Important orbitals of **2Be^{Me}**. BP86/TZ2P orbital energies.

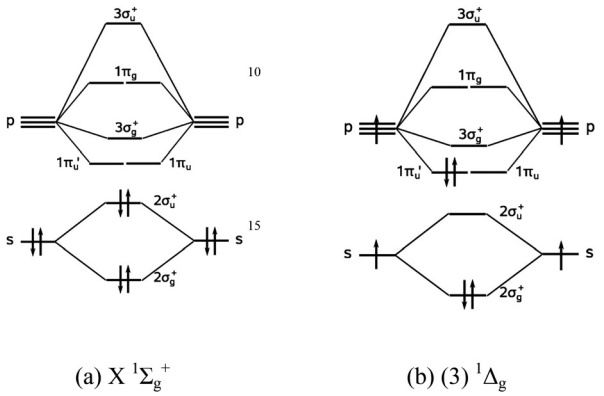

Fig. 6 Orbital correlation diagrams for the ground and third excited singlet states of Be_2 and Mg_2.

orbitals of **2Be^{Me}**. The HOMO and HOMO − 1 are π and σ orbitals, which are mainly localized at the Be_2 moiety. From the correlation diagram, which is shown in Fig. 6, it becomes obvious that the orbitals correlate with the $2\sigma_g^+$ orbital and one of the degenerate $1\pi_u$ MOs of free Be_2. The other $1\pi_u$ MO of Be_2 remains empty and becomes the LUMO of **2Be^{Me}** (Fig. 5). Thus, the electronic reference state of Be_2 in **2Be^{Me}** is the third excited (3) $^1\Delta_g$ state, which is estimated to be 268 kJ mol^{-1} above the X $^1\Sigma_g^+$ ground state.[45] Fig. 6b shows that the (3) $^1\Delta_g$ state, which has a formal Be=Be double bond, is perfectly suited for σ donation into the vacant $2\sigma_u^+$ and $3\sigma_g^+$ MOs of free Be_2. Here, the $2\sigma_u^+$ MO may receive electronic charge from the minus combination of the σ donor orbitals while $3\sigma_g^+$ MOs serves as acceptor for the plus combination. Fig. 5 shows that the HOMO − 6 and the HOMO − 7 of **2Be^{Me}** are the NHC^{Me}→Be_2←NHC^{Me} σ-donor orbitals that arise from the minus and plus donation. However, the HOMO of **2Be^{Me}** exhibits significant coefficients at the NHC^{Me} ligands, which suggests some degree of NHC^{Me}←Be_2→NHC^{Me} π backdonation.

We carried out an energy decomposition analysis (EDA) of **2Be^{Me}** in order to quantitatively estimate the strength of the σ and π orbital interactions. Table 3 shows the EDA results. The intrinsic interaction energy ΔE_{int} = −723.9 kJ mol^{-1} between (3) $^1\Delta_g$ Be_2 and 2 NHC^{Me} is quite strong. The covalent (orbital) interactions ΔE_{orb} contribute 46.7% to the total attraction. The breakdown of the latter term into orbitals with different symmetry suggests that 54.8% come from σ donation while 42.3% come from π interactions. Thus, the NHC^{Me}←Be_2→NHC^{Me} π backdonation in **2Be^{Me}** is nearly as strong as the NHC^{Me}→Be_2←NHC^{Me} σ donation.

The covalent bonding between the Be_2 moiety and the NHC^{Me} ligands in **2Be^{Me}** becomes visible by the calculated deformation densities $\Delta\rho$, which are associated with the most important orbital interactions between the fragments. The EDA-NOCV method makes it possible to calculate the individual contributions of pairwise interactions. Usually, there are only a small number of pairwise interactions that make a significant contribution to ΔE_{orb}. Fig. 7 shows three deformation densities $\Delta\rho$ and the associated energy values which provide 88.1% of the overall orbital interactions.

Visual inspection of Fig. 7a indicates that $\Delta\rho_1$ comes from the NHC^{Me}←Be_2→NHC^{Me} π backdonation, which give the largest individual pairwise contribution (−241.0 kJ mol^{-1}) to the orbital interaction. Note that the colour in Fig. 7 denotes the charge flow, which is from the red to the blue region. Fig. 7b and 7c display the deformation densities $\Delta\rho_2$ and $\Delta\rho_3$ which come from the NHC^{Me}→Be_2←NHC^{Me} σ donation that arises from the plus and minus combination of the donor orbitals. The former donation, which strengthens the Be–Be bond because the $3\sigma_g^+$ orbital of Be_2 is filled (Fig. 6a), is stronger (−190.8 kJ mol^{-1}) than the donation of the minus combination (−137.2 kJ mol^{-1}).

Further light may be shed on the nature of the Be–Be bond from multi-center Mayer-type bond order calculations, which indicate significant 3-center–2-electron (3c–2e) Be–Be–C bond character (index is 0.236, the theoretical maximum 3c–2e index is 0.296). Moreover, the WBI value of 1.32 for the Be–Be bond order in **2Be^{Me}** is consistent with the above description of the Be_2 moiety being in the $^1\Delta_g$ electronic state and possessing a bond having some multiple bond character.

Table 3 Results of the EDA calculations at BP86/TZ2P (kJ mol^{-1})

	2Be^{Me}	**2Mg^{Me}**	**4Be^{Me}**	Be(NHC^{Me})$_2$
Sym	C_{2v}	C_i	C_3	C_{2v}
ΔE_{int}	−723.9	−106.8	−1317.3	−1037.9
ΔE_{Pauli}	657.9	730.9	617.7	389.9
ΔE_{Elstat} [a]	−735.8 (53.3%)	−532.3 (63.6%)	−893.7 (46.2%)	−624.7 (43.8%)
ΔE_{orb} [a]	−645.9 (46.7%)	−305.3 (36.4%)	−1041.3 (53.8%)	−803.1 (56.2%)
ΔE_{a1} [b]	−354.2 (54.8%)	—	—	−525.5 (65.4%)
ΔE_{a2} [b]	−0.7 (0.1%)	—	—	−9.6 (1.2%)
ΔE_{b1} [b]	−273.0 (42.3%)	—	—	−251.8 (31.4%)
ΔE_{b2} [b]	−18.1 (2.8%)	—	—	−16.2 (2.0%)
ΔE_{prep}	299.6	23.4	865.3	747.2
$-D_e$	424.3	83.4	452.1	290.7

[a] The values in parentheses are the percentage contributions to the total attractive interactions $\Delta E_{elsat} + \Delta E_{orbital}$. [b] The values in parentheses are the percentage contributions to the total orbital interactions $\Delta E_{orbital}$.

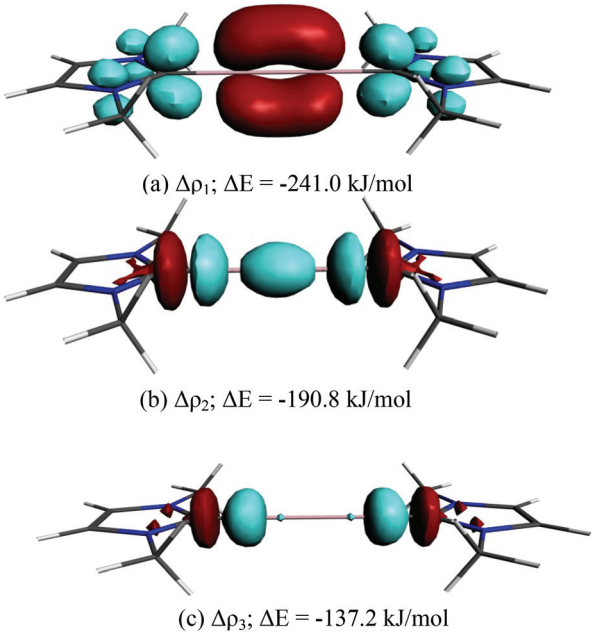

Fig. 7 Deformation densities $\Delta\rho$ associated with the most important orbital interactions in **2Be^{Me}**. The direction of the charge flow is red→blue. (a) Deformation density $\Delta\rho_1$ due to NHC^{Me}←Be_2→NHC^{Me} π backdonation. (b) Deformation density $\Delta\rho_2$ due to NHC^{Me}→Be_2←NHC^{Me} σ donation that arises from the plus combination of the donor orbitals. (c) Deformation density $\Delta\rho_2$ due to NHC^{Me}→Be_2←NHC^{Me} σ donation that arises from the minus combination of the donor orbitals.

The geometry and the shape of the most important orbitals of the magnesium homologue **2Mg^{Me}** (Fig. 8) suggests that the bonding situation is clearly different than in **2Be^{Me}**. It is obvious that the orbital interactions in **2Mg^{Me}** involve the X $^1\Sigma_g^+$ ground state of Mg_2, which has a formal bond order of zero. The acceptor orbitals of Mg_2 in the X $^1\Sigma_g^+$ ground state are the vacant in-plane π and π* orbitals (Fig. 9) which receive electronic charge from the minus and plus combinations of the donor orbitals. Fig. 8 shows that the HOMO and HOMO − 1 of **2Mg^{Me}** are the slightly distorted $2\sigma_g^+$ and $2\sigma_u^+$ orbitals of Mg_2, which are occupied in the ground state (Fig. 6a). The Mg–NHC^{Me} bonding orbitals are the HOMO − 4 and HOMO − 5 that arise from the minus and plus donation. In contrast to **2Be^{Me}**, the HOMO exhibits virtually no contribution from the NHC^{Me} ligands, which suggests there is no significant degree of NHC^{Me}←Mg_2→NHC^{Me} π backdonation.

From EDA calculations of **2Mg^{Me}** the intrinsic interaction energy ΔE_{int} = −106.8 kJ mol^{-1} between (X) $^1\Sigma_g^+$ Mg_2 and 2 NHC^{Me} and is much weaker than for **2Be^{Me}**. The covalent (orbital) interactions ΔE_{orb} contribute 36.4% of the total attraction, which is significantly less than that for **2Be^{Me}** (46.7%) and is consistent with a weaker Mg–ligand interaction in **2Mg^{R}**.

For **3Be^{Me}**, $(NHC^{Me})_2$–Be_2–$(NHC^{Me})_2$, the most important MOs are shown in Fig. 10. The HOMO − 1 of **3Be^{Me}** is dominated by a Be–Be σ bond. The 3c–2e bond index for Be–Be–C is 0.136, again indicative of some delocalization.

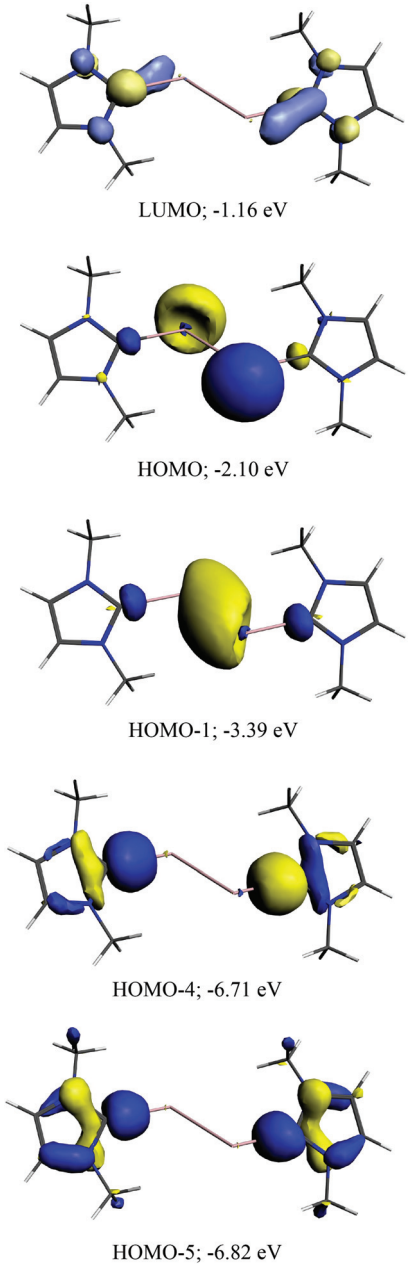

Fig. 8 Important orbitals of **2Mg^{Me}**. BP86/TZ2P energies.

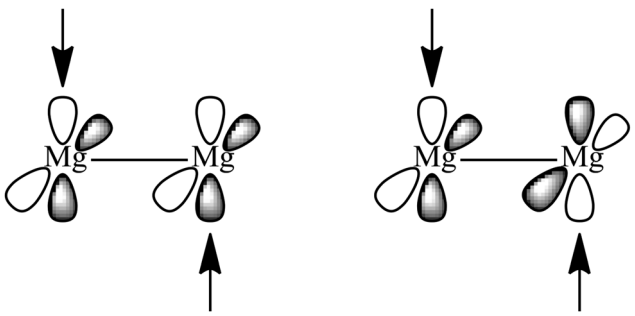

Fig. 9 Schematic representation of the donor–acceptor interactions in **2Mg^{Me}**.

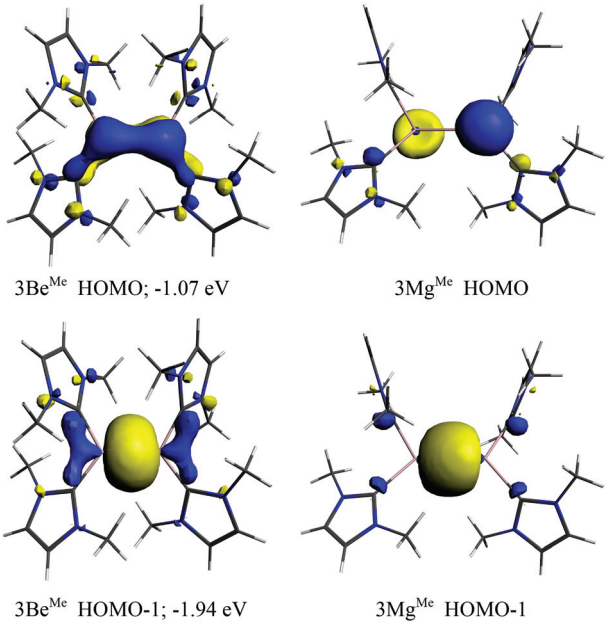

Fig. 10 Important orbitals of (a) **3Be^{Me}** and (b) **3Mg^{Me}**. BP86/TZ2P energies.

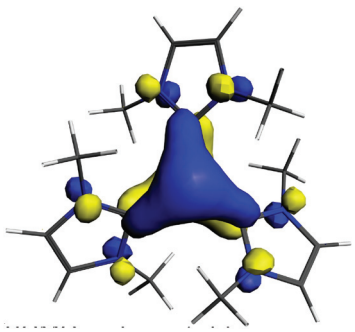

Fig. 11 HOMO of **4Be^{Me}**.

In **3Be^{Ph}**, the Be–Be π interaction is not apparent in the π symmetric HOMO, which is more localized on the NHC. The loss of some of the Be–Be bonding interaction in this derivative is apparent in the calculated geometrical parameters, with a substantially longer Be–Be bond (2.225 Å) for R = Ph, than for R = Me (2.098 Å), consistent with the facile dissociation of the Be–Be bond calculated for **3Be^{Ph}**.

For **3Mg^{Me}** the HOMO (Fig. 10) is a non-bonding orbital with an equal contribution from each Mg atom. The contraction of the Mg–Mg bond in **2Mg^{Me}** upon adding additional NHCs generating **3Mg^{Me}** can be rationalized by examination of the LUMO of **2Mg^{Me}**, which is σ symmetric and bonding with respect to the Mg–Mg interaction. No significant 3c–2e bonding is predicted for any Mg compound considered, which further illustrates the difference between Be and Mg chemistry. In any case, our thermochemical studies suggest these Mg(0) adducts will be unviable molecules in the context of an isolation in the condensed phase.

For **4Be^{R}** the HOMO is dominated by a π symmetric orbital centred on the Be atom (Fig. 11). In valance bond terms, this can be considered as a p-orbital lone pair of electrons on an sp_2 hybridized beryllium. NBO theory localizes this orbital on the Be centre with 100% p-character. MOs corresponding to the Be–C σ bonds can be found in the HOMO − 7, HOMO − 8 and HOMO − 9. This is consistent with the results in the recent Parameswaran paper, which insightfully described this compound as isostructural with a borane, but isoelectronic to an amine.[43]

Computational methods

Geometry optimisations without symmetry constraints were carried out using B3LYP-DFT.[47,48] The def2-TZVPP basis set was employed for all atoms.[49] For **3Be^{Ph}**, geometries were optimized with the def2-TZVP basis set. Stationary points were characterised as minima by calculating the Hessian matrix analytically at the same level of theory. All structures are minima with no imaginary frequencies. Thermodynamic corrections were taken from these calculations (standard state of T = 298.15 K and p = 1 atm). Single-point MP2/def2-TZVPP energies were calculated using the B3LYP/def2-TZVPP optimised geometries. Tabled MP2 energies are presented as ΔG values, which combine the MP2/def2-TZVPP electronic energy and B3LYP/def2-TZVPP thermochemical correction.

Calculations of dissociation of L–E–E–L to E_2 and L employed B3LYP/def2-TZVPP optimized E_2 and L geometries and thermal corrections along with MP2/def2-TZVPP electronic energies. A singlet ground state was used for Be_2. All L–E–E–L complexes were considered as singlet states. Triplet states of L–E–E–L compounds were all higher in energy at the MP2/def2-TZVPP level of theory.

Unless noted, calculations were carried out within Gaussian 09.[50] Mayer-type bond order index calculations were carried out within the AOMIX program[51] at the B3LYP/TZVP level of theory using the B3LYP/def2-TZVPP optimized geometries. EDA and EDA-NOCV calculations were performed using the ADF package.[52] BP86 was chosen for the application of uncontracted Slater-type orbitals (STOs) as basis functions.[53] The latter basis sets for all elements have triple-ζ quality augmented by two sets of polarization functions (ADF-basis set TZ2P). This level of theory is denoted BP86/TZ2P. An auxiliary set of s, p, d, f, and g STOs was used to fit the molecular densities and to represent the Coulomb and exchange potentials accurately in each SCF cycle.[54] Scalar relativistic effects have been incorporated by applying the zeroth-order regular approximation (ZORA) in all ADF calculations.[55]

Conclusions

We have identified *in silico* that low-valent beryllium compounds should be stable molecules and hence accessible targets for synthesis. Be–NHC chemistry is an area of increasing interest,[27,39] and the NHC stabilized Be(0)–Be(0) and monoberyllium(0) complexes considered here represent a potentially new class of molecule for s-block chemistry. Our observations of Be induced weakening of the C–N carbene

bond is of interest in the light of Hill's observation of Be insertion into an NHC C–N bond,[39] and we are currently undertaking a more detailed study of this avenue.

The calculated non-viability of the Mg analogues underscores the unique opportunities beryllium chemistry affords and we would challenge research groups who are properly equipped to safely perform such chemistry to pursue this avenue. Improved methods for safely handling the required BeX_2 halide starting materials are becoming available, hopefully making opportunities in beryllium chemistry more accessible.[46]

We thank La Trobe University and the La Trobe Institute of Molecular Science for generous financial support of this work. The Victorian Partnership for Advanced Computing (VPAC) and the National Computational Infrastructure National Facility (NCI-NF) are acknowledged for substantial computing resources. This project is supported by an Australian Research Council DECRA award (DE130100186).

Notes and references

1 R. Puchta, *Nat. Chem.*, 2011, **3**, 416.
2 N. N. Greenwood and A. Earnshaw, *Chemistry of the Elements*, Reed Educational and Professional Publishing, Oxford, 2nd edn, 1997.
3 R. Puchta, B. Neumüller and K. Dehnicke, *Z. Anorg. Allg. Chem.*, 2011, **637**, 67–72.
4 W. Petz, K. Dehnicke, N. Holzmann, G. Frenking and B. Neumuller, *Z. Anorg. Allg. Chem.*, 2011, **637**, 1702–1710.
5 G. Frenking, N. Holzmann, B. Neumüller and K. Dehnicke, *Z. Anorg. Allg. Chem.*, 2010, **636**, 1772–1789.
6 K. Dehnicke and B. Neumüller, *Z. Anorg. Allg. Chem.*, 2008, **634**, 2703–2728.
7 S. Li, X. Yang, Y. Liu, Y. Zhao, Q. Li, Y. Xie, H. F. Schaefer III and B. Wu, *Organometallics*, 2011, **30**, 3113–3118.
8 A. Velazquez, I. Fernandez, G. Frenking and G. Merino, *Organometallics*, 2007, **26**, 4731–4736.
9 S. P. Green, C. Jones and A. Stasch, *Science*, 2007, **318**, 1754–1757.
10 A. Sidiropoulos, C. Jones, A. Stasch, S. Klein and G. Frenking, *Angew. Chem., Int. Ed.*, 2009, **48**, 9701–9704.
11 A. Stasch and C. Jones, *Dalton Trans.*, 2011, **40**, 5659–5672.
12 C. A. Dyker and G. Bertrand, *Science*, 2008, **321**, 1050–1051.
13 Y. Wang and G. H. Robinson, *Dalton Trans.*, 2012, **41**, 337–345.
14 Y. Wang, Y. Xie, P. Wei, R. B. King, H. F. Schaefer III, P. v. R. Schleyer and G. H. Robinson, *Science*, 2008, **321**, 1069–1071.
15 C. Jones, A. Sidiropoulos, N. Holzmann, G. Frenking and A. Stasch, *Chem. Commun.*, 2012, **48**, 9855–9857.
16 Y. Wang, Y. Xie, P. Wei, R. B. King, H. F. Schaefer III, P. v. R. Schleyer and G. H. Robinson, *J. Am. Chem. Soc.*, 2008, **130**, 14970–14971.
17 M. Y. Abraham, Y. Wang, Y. Xie, W. Pingrong, H. F. Schaefer III, P. v. R. Schleyer and G. H. Robinson, *Chem.–Eur. J.*, 2009, **16**, 432–435.
18 N. Holzmann, A. Stasch, C. Jones and G. Frenking, *Chem.–Eur. J.*, 2011, **17**, 13517–13525.
19 J. L. Dutton and D. J. D. Wilson, *Angew. Chem., Int. Ed.*, 2012, **51**, 1477–1480.
20 D. J. D. Wilson, S. Couchman and J. L. Dutton, *Inorg. Chem.*, 2012, **51**, 7657–7668.
21 H. Braunschweig, R. D. Dewhurst, K. Hammond, J. Mies, K. Radacki and A. Vargas, *Science*, 2012, **336**, 1420–1422.
22 R. Tonner and G. Frenking, *Angew. Chem., Int. Ed.*, 2007, **46**, 8695–8698.
23 C. A. Dyker, V. Lavallo, B. Donnadieu and G. Bertrand, *Angew. Chem., Int. Ed.*, 2008, **47**, 3206–3209.
24 J. M. Merritt, V. E. Bondybey and M. C. Heaven, *Science*, 2009, **324**, 1548–1551.
25 K. Patkowski, V. Spirko and K. Szalewicz, *Science*, 2009, **326**, 1382–1384.
26 W. A. Herrmann, O. Runte and G. Artus, *J. Organomet. Chem.*, 1995, **501**, C1–C4.
27 R. J. J. Gillard, M. Y. Abraham, Y. Wang, P. Wei, Y. Xie, B. Quillian, H. F. Schaefer III, P. v. R. Shleyer and G. H. Robinson, *J. Am. Chem. Soc.*, 2012, **134**, 9953–9955.
28 H. Clavier and S. P. Nolan, *Chem. Commun.*, 2010, **46**, 841–861.
29 G. Berthon-Gelloz, M. A. Siegler, A. L. Spek, B. Tinant, J. N. H. Reek and I. E. Marko, *Dalton Trans.*, 2010, **39**, 1444–1446.
30 Derivatives with –H, –Me and –Ph substituents will calculated. In all cases in this study the metrical parameters changed very slightly with differing substitutions. Discussion in the manuscript is confined to the –Me derivatives for purposes of clarity and brevity.
31 J. Sheu and M. Su, *J. Organomet. Chem.*, 2011, **696**, 1221–1227.
32 S. J. Bonyhady, C. Jones, S. Nembenna, A. Stasch, A. J. Edwards and G. J. McIntyre, *Chem.–Eur. J.*, 2010, **16**, 938–955.
33 M. Arrowsmith, M. S. Hill, G. Kohn-Kociok, D. J. MacDougall, M. F. Mahon and I. Mallov, *Inorg. Chem.*, 2012, **51**, 13408–13418.
34 K. K. Sunil, *J. Am. Chem. Soc.*, 1992, **114**, 3985–3986.
35 L. Andrews, T. J. J. Tague, G. P. Kushto and R. D. Davy, *Inorg. Chem.*, 1995, **34**, 2952–2961.
36 T. Kar, P. K. Nandi and A. B. Sannigrahi, *Chem. Phys. Lett.*, 1994, **220**, 133–137.
37 A. B. Sannigrahi and T. Kar, *J. Mol. Struct.*, 2000, **496**, 1–17.
38 N. Frohlich, U. Pidun, M. Stahl and G. Frenking, *Organometallics*, 1997, **16**, 442–448.
39 M. Arrowsmith, M. S. Hill, G. Kohn-Kociok, D. J. MacDougall and M. F. Mahon, *Angew. Chem., Int. Ed.*, 2012, **51**, 2098–2100.
40 Optimized geometries for the Mg(0)–NHC complexes are found in the supporting information.
41 G. Frenking and R. Tonner, *Pure Appl. Chem.*, 2009, **81**, 597–608.

42 G. Frenking and R. Tonner, *WIREs Comput. Mol. Sci.*, 2011, **1**, 869–877.
43 S. De and P. Parameswaran, *Dalton Trans.*, 2013, **42**, 4650–4656.
44 R. Hoffman, P. v. R. Shleyer and H. F. Schaefer III, *Angew. Chem., Int. Ed.*, 2008, **47**, 7164–7167.
45 M. Pecul, M. Jaszunski, H. Larsen and P. Jørgensen, *J. Chem. Phys.*, 2000, **112**, 3671–3679.
46 D. Himmel and I. Krossing, *Z. Anorg. Allg. Chem.*, 2006, **632**, 2021–2023.
47 A. D. Becke, *Phys. Rev. A*, 1988, **38**, 3098–3100.
48 C. Lee, W. Yang and R. G. Parr, *Phys. Rev. B: Condens. Matter*, 1988, **37**, 785–789.
49 F. Weigend and R. Ahlrichs, *Phys. Chem. Chem. Phys.*, 2005, **7**, 3297.
50 M. J. Frisch, G. W. Trucks, H. B. Schlegel, G. E. Scuseria, M. A. Robb, J. R. Cheeseman, G. Scalmani, V. Barone, B. Mennucci, G. A. Petersson, H. Nakatsuji, M. Caricato, X. Li, H. P. Hratchian, A. F. Izmaylov, J. Bloino, G. Zheng, J. L. Sonnenberg, M. Hada, M. Ehara, K. Toyota, R. Fukuda, J. Hasegawa, M. Ishida, T. Nakajima, Y. Honda, O. Kitao, H. Nakai, T. Vreven, J. J. A. Montgomery, J. E. Peralta, F. Ogliaro, M. Bearpark, J. J. Heyd, E. Brothers, K. N. Kudin, V. N. Staroverov, R. Kobayashi, J. Normand, K. Raghavachari, A. Rendell, J. C. Burant, S. S. Iyengar, J. Tomasi, M. Cossi, N. Rega, J. M. Millam, M. Klene, J. E. Knox, J. B. Cross, V. Bakken, C. Adamo, J. Jaramillo, R. Gomperts, R. E. Stratmann, O. Yazyev, A. J. Austin, R. Cammi, C. Pomelli, J. W. Ochterski, R. L. Martin, K. Morokuma, V. G. Zakrzewski, G. A. Voth, P. Salvador, J. J. Dannenberg, S. Dapprich, A. D. Daniels, Ö. Farkas, J. B. Foresman, J. V. Ortiz, J. Cioslowski and D. J. Fox, *GAUSSIAN 09 (Revision A.1)*, Gaussian, Inc., Wallingford CT, 2009.
51 S. I. Gorelsky, University of Ottawa, 2011.
52 E. J. Baerends, T. Ziegler, J. Autschbach, D. Bashford, A. Bérces, F. M. Bickelhaupt, C. Bo, P. M. Boerrigter, L. Cavallo, D. P. Chong, L. Deng, R. M. Dickson, D. E. Ellis, M. van Faassen, L. Fan, T. H. Fischer, C. Fonseca Guerra, A. Ghysels, A. Giammona, S. J. A. van Gisbergen, A. W. Götz, J. A. Groeneveld, O. V. Gritsenko, M. Grüning, S. Gusarov, F. E. Harris, P. van den Hoek, C. R. Jacob, H. Jacobsen, L. Jensen, J. W. Kaminski, G. van Kessel, F. Kootstra, A. Kovalenko, M. V. Krykunov, E. van Lenthe, D. A. McCormack, A. Michalak, M. Mitoraj, J. Neugebauer, V. P. Nicu, L. Noodleman, V. P. Osinga, S. Patchkovskii, P. H. T. Philipsen, D. Post, C. C. Pye, W. Ravenek, J. I. Rodríguez, P. Ros, P. R. T. Schipper, G. Schreckenbach, J. S. Seldenthuis, M. Seth, J. G. Snijders, M. Solà, M. Swart, D. Swerhone, G. te Velde, P. Vernooijs, L. Versluis, L. Visscher, O. Visser, F. Wang, T. A. Wesolowski, E. M. van Wezenbeek, G. Wiesenekker, S. K. Wolff, T. K. Woo and A. L. Yakovlev, *ADF2012, SCM, Theoretical Chemistry*, Vrije Universiteit, Amsterdam, The Netherlands, http://www.scm.com
53 J. G. Snijders, E. J. Baerends and V. P., *At. Data Nucl. Data Tables*, 1981, **26**, 483–509.
54 J. Krijn and E. J. Baerends, *Fit Functions in the HFS-Method: Internal Report (in Dutch)*, Vrije Universiteit Amsterdam, The Netherlands, 1984.
55 E. Van Lenthe, E. J. Baerends and J. G. Snijders, *J. Chem. Phys.*, 1993, **99**, 4597–4610.

